Calculated rates for the electron impact dissociation of molecular hydrogen, deuterium and tritium

Cynthia S. Trevisan and Jonathan Tennyson

Department of Physics and Astronomy, University College London, Gower St., London WC1E 6BT, UK.

Abstract. At temperatures below 15,000 K, the major pathway for the electron impact dissociation of H_2 is through excitation to the b $^3\Sigma_u^+$ excited electronic state. Total cross sections and energy differential cross sections for threshold energies as a function of vibrational states (v) for H_2 $v = 0 - 4$, D_2 $v = 0 - 6$ and T_2 $v = 0 - 7$ are calculated. The rates of dissociation as a function of electron temperature for each state are parametrized. Near-threshold rates are shown to be so critically dependent on the vibrational level that dissociation from very high-lying vibrational levels must be included in calculations of the rate at local thermal equilibrium (LTE) even at low temperature. An adapted version of the extrapolation procedure of Stibbe and Tennyson (1999, Astrophys. J., 513:L147) is used to approximate the rates for all of the higher vibrational levels, which are then used to calculate the LTE rate. The LTE rate is an order of magnitude greater than the $v = 0$ rate. Calculations of energy differential cross sections suggest that impact dissociation of vibrationally excited molecules could be the source of low energy H atoms observed in tokamak plasmas.

1. Introduction

In order to understand the role of collision processes in plasmas and their effects on plasma properties and dynamics, it is essential to have an in depth knowledge of the physics of these processes and detailed information on their quantitative characteristics (transition rates, cross sections, reaction rates coefficients, etc.). Modelling of cool plasmas requires the knowledge of a large number of cross sections involving electron-molecule interactions (electronic excitation, dissociation, and ionization). A lot of information, both experimental and theoretical, has been obtained to this end. Experimentally, many cross sections have been obtained from investigations of electron-molecule interactions in cross-beams experiments (Erhardt 1990), as well as by deconvolution of transport properties by a Boltzmann analysis of swarm data (Hayashi 1990). Theoretically, many quantum mechanical methods including resonance theories, close-coupling methods, distorted-wave approximations, and variational methods, have been developed (Bardsley 1990, Burke 1993). Most of these data, however, refer to the various processes involving the ground vibrational state of H_2 and D_2 molecules so that their use is limited to very cool plasmas in which the presence of vibrationally excited molecules can be neglected.

Under many circumstances, such as multicusp magnetic plasmas or fusion edge plasmas, the vibrational excitation of H_2, D_2 and T_2 cannot be neglected, so that complete sets of cross sections involving the whole vibrational manifold of the diatoms should be known (Capitelli & Celiberto 1995). Indeed, subtle effects in the detailed physics can have consequences for the plasma. For example, the source of many low energy H atoms observed in tokamak plasmas (Mertens et al. 2001, Tanaka et al. 2000, Hey et al. 2000) remains unexplained.

Experimentally it is difficult to measure cross sections (or rates) for electron impact dissociation of a neutral species into neutral fragments. Only limited experimental data is available for this process (Corrigan 1965, Khakoo & Segura 1994, Nishimura & Danjo 1986, Hall & Andrić 1984), all of it for H_2 in its $v = 0$ vibrational ground state. However, calculations by Stibbe and Tennyson (1998*a*, 1999) have shown that the rate of near threshold electron impact dissociation is strongly dependent on the initial vibrational state of H_2. The information about cross sections involving vibrationally excited states comes from theoretical considerations.

Recently, an extensive database of cross sections for inelastic electron-impact processes of vibrationally excited hydrogen and its isotopes has been compiled by Celiberto *et al* (2001). Cross sections reported for the singlet-triplet transition $X^1\Sigma_g^+ \rightarrow b^3\Sigma_u^+$ were obtained using a semiclassical method (Celiberto et al. 1989, Bauer & Bartky 1965) for H_2 and D_2. This method should give satisfactory results at high impact electron energies and hence temperatures, but is not reliable in the near-threshold (low temperature) regime were subtle quantum effects must be correctly modelled.

In this paper we present the total cross sections, energy differential cross sections and rates for electron impact dissociation of H_2, D_2 and T_2 as a function of the vibrational states. We use the adiabatic nuclei approximation and the energy balance model of Stibbe and Tennyson (1998*a*) to obtain the appropriate energy-dependent T-matrices. This model assumes that the dissociation of H_2 for energies below around 12eV proceeds exclusively via electronic excitation to the first excited state of H_2:

$$e + H_2(X^1\Sigma_g^+) \rightarrow H_2^*(b^3\Sigma_u^+) + e \rightarrow H(1s) + H(1s) + e. \qquad (1)$$

We have recently derived the formal expressions needed for such calculations and presented total and differential cross sections for the electronic ground state vibrational level $v = 0$ of H_2 (Trevisan & Tennyson 2001). To generate differential cross sections we were led to rederive the expressions for all cross sections from first principles. We found problems with Stibbe and Tennyson's formula for the cross sections which arose from not having considered the density of final states. We note that this term introduces a mass dependence in all dissociation processes which is important for present work. This reformulation, thus, gives results which differ somewhat both in magnitude and energy dependence from the earlier results of Stibbe and Tennyson (1998*a*, 1999). Our total cross sections for this process are in good agreement with the limited experimental data available, all of which is for the $v = 0$ vibrational state. Here we extend these calculations to the $v = 0 - 4$ H_2, $v = 0 - 6$ D_2 and $v = 0 - 7$ T_2 vibrational states,

produce rates for such vibrational states and adapt the extrapolation procedure of Stibbe and Tennyson (1999) to approximate the rates for all of the higher vibrational levels, which we then use to calculate the LTE rates.

2. Method and Results

The T-matrices used here were originally calculated in an investigation of H_2^- resonances as a function of the internuclear distance R (Stibbe and Tennyson 1997*a*, 1997*b*, 1998*b*). Such geometry-dependent, off-shell fixed-nuclei T-matrices were averaged between wave functions for the ground vibrational states and nuclear motion continuum functions with appropriate energy to represent the dissociating state. This generalization of the adiabatic nuclei approximation to electron impact dissociation is discussed in detail by Stibbe and Tennyson (1998*a*). The formal expressions needed for the calculation of differential and total cross sections were developed in our previous study (Trevisan & Tennyson 2001). For the energy differential cross sections we have‡

$$\frac{\mathrm{d}\sigma}{\mathrm{d}E_{ke}} = \frac{M}{4\pi^3 m_e}\frac{E_{ke}}{E_{in}}\sum_{\Lambda\nu l_i l_j}\left|T^{\Lambda\nu}_{\bar{i}\bar{l}_i\bar{j}\bar{l}_j}(E_{in},E_{out})\right|^2 \tag{2}$$

where M represents the atomic mass, m_e is the mass of the electron, E_{in} the incoming electron energy, E_{ke} the energy of the dissociating atoms and E_{out} the energy of the scattered electron. $T^{\Lambda\nu}_{\bar{i}\bar{l}_i\bar{j}\bar{l}_j}(E_{in},E_{out})$ are the transition matrix elements, where the indices i, j label the initial and final electronic states of the molecule and represent all quantum numbers needed to specify the electronic state i, j of the molecule, respectively. $\bar{i}$,$\bar{j}$ stand for (Λ_i, S_i, ν_i) and (Λ_j, S_j, ν_j), and $\bar{l}_i$,$\bar{l}_j$ run over values satisfying $(-1)^{\bar{l}_i}\nu_i = \nu$; $(-1)^{\bar{l}_j}\nu_j = \nu$; Λ is the projection of the total electronic angular momentum on the internuclear axis; S represents the total spin and ν labels the gerade or ungerade symmetry in homonuclear molecules.

The mass dependance in eq. (2) comes from considering the density of final states for a three body problem in the output channel. Because its derivation is independent of any particular electronic state, we expect the same scaling of cross sections for all dissociation processes as a function of the isotopic mass.

Nuclear continuum wavefunctions, $\Xi_c(E_{ke},R)$, were calculated by directly solving the Schrödinger equation for the dissociating potential, and energy normalized. The potential of Kolos and Wolniewicz (1965) was used in place of that implicit in the T-matrix calculations, which is ($\sim$ 0.1 eV) less accurate. The initial vibrational wavefunctions, $\Xi_v(R)$, and energies were found with the program LEVEL (LeRoy 1996) also using the former potential.

Total cross sections are given by

$$\sigma(E_{in}) = \int_0^{E_{in}-D_v}\frac{\mathrm{d}\sigma}{\mathrm{d}E_{ke}}dE_{ke} \tag{3}$$

‡ Please note that the summation indices in (Trevisan & Tennyson 2001) should read $\Lambda\nu l_i l_j$ instead of $\Lambda\nu l_i l j$ in eq. (29), (30) and (35).

with D_v the vibrational state-dependent dissociation energy. No allowance is made for the possible effect of rotational motion of the diatoms.

Figures 1 to 3 show the dissociation cross sections for $H_2(v)$, $D_2(v)$ and $T_2(v)$ as a function of incoming electron energy. Although cross sections are shown up to values of E_{in} that go beyond 12 eV, our calculations are expected to be accurate only up to around that value. Above that energy, the molecule can be excited to higher states from which it can dissociate directly or cascade down to the repulsive state. Another possibility above 12 eV is the excitation of an H_2 resonance state which can then decay into the b $^3\Sigma_u^+$ state. The adiabatic model we use is not valid for these long-lived resonances and the additional dissociation pathways above 12 eV are not included in our model.

Comparison of Celiberto *et al* (2001) results with our calculations for H_2 and D_2 are shown in figures 1 and 2, respectively, where total cross sections are plotted against the energy of the incoming electron for all the vibrational states that we are able to calculate fully. Cross sections calculated by Celiberto *et al* appear to be lower than the ones in our calculation, with a more noticeable effect in the case of D_2.

Because of the finite range of internuclear separations (R=0.8-4.0 a_o) for which T-matrices are available, full calculations are only possible for $v \leq 4$ in $H_2(v)$, $v \leq 6$ in $D_2(v)$ and $v \leq 7$ in $T_2(v)$. In order to obtain accurate cross sections for higher vibrational states, T-matrices must be calculated over a much wider range of bond length. Our present calculation cannot be extended to provide these T-matrices because of basis set limitations and because, at long bond length, the target electronic wave function will leak out of the R-matrix boundary.

Figures 4 to 6 illustrate energy differential cross sections contour plots for the different isotopes and for each of the initial bound vibrational wavefunction for which our T-matrices were able to support full calculations. The energy of the dissociating atoms, E_{ke} is plotted against the electron impact energy, E_{in}; values for a single atom can be obtained by halving E_{ke}. At low energies for the incoming electron (below 12 eV), contour plots for the $v = 0$ vibrational state show that most of the available energy above dissociation is carried away by the dissociating atoms. This suggests that the electron impact dissociation from such vibrational state is unlikely to be the source of anomalously cold H atoms which have been found in a number of hydrogen plasmas (Hey *et al* 1996, 1999, 2000, Mertens and Silz 1997). Nevertheless, these contour plots also show that, for dissociation from higher vibrational states, the heavy particles' energy E_{ke} is only weakly dependent on E_{in}. The distribution of E_{ke} becomes narrower, and its mean value becomes lower for dissociation from excited vibrational levels. This finding is in accordance with predictions that low energy dissociation is predominantly from the outer turning point of the H_2 ground state potential. It could explain the presence of cold atoms which originate from electron impact dissociation from higher vibrational states.

The rate of electron impact dissociation of the diatom in vibrational state v as a function of electron temperature T_e is calculated from the relevant cross sections using

the standard formula

$$q_v(T_e) = \frac{8\pi}{m_e^{1/2}} \left(\frac{1}{2\pi k T_e} \right)^{3/2} \int_0^\infty \sigma_v(E) e^{-E/kT_e} E dE \tag{4}$$

where k is the Boltzmann constant and m_e is the electron mass. For the temperatures under consideration here (up to 15,000 K), the threshold region of dissociation provides by far the larger contribution to the total rate. The upper limit for the integral in eq. (4) of 15 eV should give an accurate rate at temperatures below 15,000 K.

Stibbe and Tennyson (1999) found a strong dependence of H_2 rates on the initial vibrational level. They proposed an extrapolation procedure to approximate the rates for all the vibrational levels above the ones provided by full T-matrices calculations. In this procedure, the fixed nuclei T-matrices used in the full calculation of the nuclear motion averaged T-matrices are replaced by a constant obtained by fitting Franck-Condon results for the cross sections of the lower vibrational states to those of the full calculation as closely as possible in the threshold region (see Stibbe and Tennyson, 1999, figure 1). For higher vibrational states, such Franck-Condon calculations can be used to model the cross sections near threshold without the need for further fixed nuclei T-matrix calculations.

This approximation should be useful, because the contribution from a $v = n$ level will be most significant in the region near its threshold. Beyond that region, the contribution due to the next lower vibrational state should predominate. Stibbe and Tennyson (1999) assumed that the contribution of a particular vibrational state to the total dissociation rate should be negligible beyond the threshold region and used the Franck-Condon fitted results directly in the calculation of rates of the higher vibrational states. Away from threshold the estimated cross sections are always lower than the ones obtained by full calculations, the rates calculated using this approximation will consistently underestimate the true values.

In order to test the validity of this extrapolation procedure, we chose a value for the estimated cross sections beyond which the actual cross sections should have a small contribution to the calculation of rates. This value was chosen above the threshold for the $v = n - 1$ state such that the contribution of the cross sections of the $v = n$ vibrational state should be dwarfed by it. In this way, each vibrational state determines the point at which its previous (higher) vibrational state contributes significantly for the $v = n$ state. Beyond that point, we doubled the estimated values obtained by our Franck-Condon calculations and recalculated the dissociation rates. The results shown in figures 7 to 9 are those obtained by performing calculations at a mid-point between the original Franck-Condon fits and the ones produced after doubling the estimated cross section "tails". The maximum differences found by this procedure were of about 25%. At temperatures below 10,000 K, the differences, which are temperature dependent, vary between approximately 0% and 20%. This relaxes the initial assumption of Stibbe and Tennyson (1999) and establishes an error estimation for it. This analysis also serves to emphasize the point that the reliability of our rates drops with temperature.

Following this procedure, we extrapolated thermal rates for the higher vibrational levels $5 \leq v \leq 14$ in $H_2(v)$, $7 \leq v \leq 20$ in $D_2(v)$ and $8 \leq v \leq 25$ in $T_2(v)$. Figures 7 to 9 show both the calculated (solid lines) and extrapolated (dashed lines) rates and the local thermal equilibrium rate (dash-dot line). Our H_2 rates are lower than those calculated by Stibbe and Tennyson (1999), with differences increasing with v: rates practically coincide for $v = 0$, but get progressively smaller as v increases. Our LTE rate is almost an order of magnitude lower than the LTE rate calculated by Stibbe and Tennyson. The reason for this is that, although we used the same T-matrices, our formulation (Trevisan & Tennyson 2001) led to a significantly different expression for the energy differential cross sections. The resulting total cross sections were approximately 10% higher than those obtained by Stibbe and Tennyson for H_2 $v = 0$, but reach lower maximum values for higher vibrational states. Nevertheless, we found the dependence on the initial vibrational level to be strong. This is significant when considering total rates for a particular distribution of molecules among its vibrational levels. The $v = 0$ value for the rate is often used to approximate the total dissociation rate. However, the v dependence is so critical that this is unlikely to be a good approximation in many situations.

The rates (in cm^3s^{-1}) are parametrized to the form

$$q(T) = aT^b exp\left(-\frac{c}{T}\right) \times 10^{-9} \tag{5}$$

and the parameters are given in Table 1. Although we do not have a formal statistical deviation for our fits, the difference tolerance is guaranteed to be below 0.01%.

Table 1. Parameters for the fit formula of the electron impact dissociation rates in cm^3s^{-1} for $v \leq 4$ in $H_2(v)$, $v \leq 6$ in $D_2(v)$ and $v \leq 7$ in $T_2(v)$ assuming a thermal electron distribution, and the LTE rate for each diatom. T_{min} is the cutoff temperature below each rate is under 10^{-14} cm^3s^{-1} and effectively zero.

	T_{min} (K)	a	b	c
H_2 $v=0$	7250	4.4886	0.109127	101858.0
H_2 $v=1$	6100	5.6559	0.069444	85371.7
H_2 $v=2$	5200	2.1755	0.149128	71582.2
H_2 $v=3$	4450	0.9581	0.217141	60136.4
H_2 $v=4$	3800	0.4223	0.285661	50186.9
H_2 LTE	4050	1.9075	0.135953	53407.1
D_2 $v=0$	7100	8.2424	0.126016	105388.0
D_2 $v=1$	6250	8.2190	0.108239	91822.9
D_2 $v=2$	5550	13.1714	0.052483	82016.1
D_2 $v=3$	5000	4.9716	0.136961	72087.1
D_2 $v=4$	4450	3.1896	0.171577	63916.3
D_2 $v=5$	3950	1.6978	0.224541	56357.2
D_2 $v=6$	3550	1.4574	0.223280	49589.8
D_2 LTE	3950	2.7463	0.163009	53339.7
T_2 $v=0$	7050	9.1702	0.158626	106722.0
T_2 $v=1$	6300	11.6580	0.118208	95155.5
T_2 $v=2$	5700	8.1872	0.141355	85471.7
T_2 $v=3$	5200	7.7082	0.139217	77595.4
T_2 $v=4$	4750	7.9320	0.129588	70766.5
T_2 $v=5$	4350	5.6860	0.154948	64182.4
T_2 $v=6$	3950	2.7986	0.216702	57711.3
T_2 $v=7$	3600	1.5883	0.265070	51883.9
T_2 LTE	3950	3.7208	0.152265	54820.6

At local thermal equilibrium (LTE), the molecules and the electrons each have a Maxwellian distribution associated with the same temperature T. The LTE rate q_{LTE} can be found from the thermally averaged cross section $\overline{\sigma}(E)$,

$$q_{LTE}(T) = \frac{8\pi}{m_e^{1/2}} \left(\frac{1}{2\pi kT}\right)^{3/2} \int_0^\infty \overline{\sigma}(E) e^{-E/kT} E dE \tag{6}$$

where

$$\overline{\sigma}(E) = \frac{1}{z} \sum_{v=0} \sigma_v(E) e^{-\gamma(v)/kT} \tag{7}$$

with z the partition function, $z = \sum_{v=0} e^{-\gamma(v)/kT}$ and $\gamma(v)$ the vibrational energy levels, with the sums running over the finite number of vibrational states. Alternatively, the rates themselves can be thermally averaged:

$$q_{LTE}(T) = \frac{1}{z} \sum_{v=0} q_v(T) e^{-\gamma(v)/kT} \tag{8}$$

The Franck-Condon cross sections were calculated using the H_2 potential curve of Kolos and Wolniewicz (1965) for all of the vibrational states. Rates were calculated using eq. (4) with cross sections obtained from our full T-matrices calculations and from the Franck-Condon factor cross sections for those states for which full calculations are not possible; they are illustrated in figures 7 to 9. These rates were put into eq. (8) to find the LTE rate for each molecule. The LTE rates are also illustrated in figures 7 to 9 and parametrized in Table 1.

Comparison between the LTE rates of the three diatoms show a near overlap between the H_2 and T_2 curves. This is the result of two compensating effects: H_2 tunnels more easily and therefore has a lower threshold; conversely, the mass factor in eq. (2) means that the higher energy cross sections for T_2 should be three times that of H_2. It would appear that for the temperatures of interest the effects nearly cancel.

3. Conclusions

There is very limited data available for the low energy electron impact dissociation from vibrationally excited states of H_2 and D_2, and none for T_2. We have calculated accurately the rate of dissociation for $v \leq 4$ in $H_2(v)$, $v \leq 6$ in $D_2(v)$ and $v \leq 7$ in $T_2(v)$ and found that the rate increases so dramatically with v that all of the initial vibrational levels must be included in a calculation of the rate at local thermal equilibrium.

From the results of the vibrational states for which we can perform full calculations, we adapt the procedure introduced by Stibbe and Tennyson (1999) to estimate the rates of dissociation from the remaining vibrational levels, $5 \leq v \leq 14$ in $H_2(v)$, $7 \leq v \leq 20$ in $D_2(v)$ and $8 \leq v \leq 25$ in $T_2(v)$. The LTE rates for each molecule were calculated from these rates and found to be at least an order of magnitude greater than the $v = 0$ rates. The fact that the LTE rates are so much higher than the $v = 0$ rates is important given that, with the lack of any alternative, the $v = 0$ rates are likely to be used as approximations to the LTE rates.

The cross sections depend on the isotope's mass and, hence, our calculated rates will also be sensitive to the specific diatom considered. Nevertheless, because of the Boltzmann distribution assumed among the vibrational levels, such mass effect will be less noticeable when calculating dissociation rates than in the actual dissociation cross sections.

There has been Doppler and laser measurements of velocity distributions of H and D atoms in the edge of fusion plasmas which have revealed the existence of cold atoms (Mertens et al. 2001, Tanaka et al. 2000, Hey et al. 2000). The electron impact dissociation of vibrationally excited molecules is a possible source of such atoms. Our energy differential cross section peaks can be used to model and predict the distribution of atomic velocities providing, thus, a possible explanation regarding the origin of these low energy atoms. They can also be used to compute plasma momentum transfer by neutral particles arising from the electron impact dissociation of H_2 and its isotopes for different initial vibrational states.

4. Acknowledgements

We wish to thank Jimena Gorfinkiel and Thornton Greenland for useful discussions and guidance.

Bardsley J N 1990 *Nonequilibrium Processes in Partially Ionized Gases* Vol. B220,p.1 M. Capitelli and J. N. Bardsley, eds., Plenum Press New York.

Bauer E & Bartky C D 1965 *J. Chem. Phys.* **43**, 2466.

Burke P G 1993 *The Physics of Electronic and Atomic Collisions* Vol. p.26 AIP Conf. Proc.,No.295, American Institute of Physics New York.

Capitelli M & Celiberto R 1995 *Atomic and Molecular Processes in Fusion Edge Plasmas* R. K. Janev, Plenum Press New York and London.

Celiberto R, Cacciatore M, Capitelli M & Gorse C 1989 *Chem. Phys.* **133**, 355.

Celiberto R, Janev R K, Laricchiuta A, Capitelli M, Wadehra J M& D. Atems E 2001 *At. Data and Nucl. Data Tables* **77**, 161-213.

Corrigan S J B 1965 *J. Chem. Phys.* **43**, 4381–4386.

Erhardt H 1990 *Nonequilibrium Processes in Partially Ionized Gases* Vol. B220,p.19 M. Capitelli and J. N. Bardsley, eds., Plenum Press New York.

Hall R I & Andrić L 1984 *J. Phys. B: At. Mol. Phys.* **17**, 3815–3825.

Hayashi M 1990 *Nonequilibrium Processes in Partially Ionized Gases* Vol. B220,p.333 M. Capitelli and J. N. Bardsley, eds., Plenum Press New York.

Hey J D, Chu C C & Hintz E 2000 *Contrib. Plasma Phys.* **40, 1-2**, 9–22.

Hey J. D, Chu C. C & Hintz E 1999 *J. Phys. B: At. Mol. Opt. Phys.* **32:(14)** 3555-3573

Hey J. D, Korten M, Lie Y. T, Pospieszczyk A, Rusbueldt D, Schweer B, Unterberg B, Wienbeck J & Hintz E 1996 *Contrib. Plasma Phys.* **36:(5)** 583-604

Khakoo M A & Segura J 1994 *J. Phys. B: At. Mol. Opt. Phys.* **27**, 2355–2368.

Kolos W and Wolniewicz L 1965 *J. Chem. Phys.* **43** 2429

LeRoy R 1996 *University of Waterloo Chemical Physics Research Report* **CP-555R**, 1.

Mertens P, Brezinsek S, Greenland P T, Hey J D, Pospieszczyk A, Reiter D, Samm U, Schweer Sergienko G & Vietzke E 2001 *Plasma Phys. Control. Fusion* **43** A349–A373

Mertens P & Silz M 1997 *J. Nucl. Materials* **241-243** 842-847

Nishimura H & Danjo A 1986 *J. Phys. Soc. Japan* **55,9**, 3031–3036.

Stibbe D. T & Tennyson J 1997*a* *Phys. Rev. Lett.* **79** 4116

Stibbe D. T & Tennyson J 1997*b* *J. Phys. B: At. Mol. Opt. Phys.* **30** L301

Stibbe D. T & Tennyson J 1998*a* *New J. Phys.* **1** 2.1-2.9

Stibbe D. T & Tennyson J 1998*b* *J. Phys. B: At. Mol. Opt. Phys.* **31** 815

Stibbe D. T & Tennyson J 1999 *Astrophys. J.* **513** L147-L150

Tanaka S, Xiao B, Kazuki K & Morita M 2000 *Plasma Phys. Control. Fusion* **42**, 1091–1103.

Trevisan C S & Tennyson J 2001 *J. Phys. B: At. Mol. Opt. Phys.* **34**, 2935–2949.

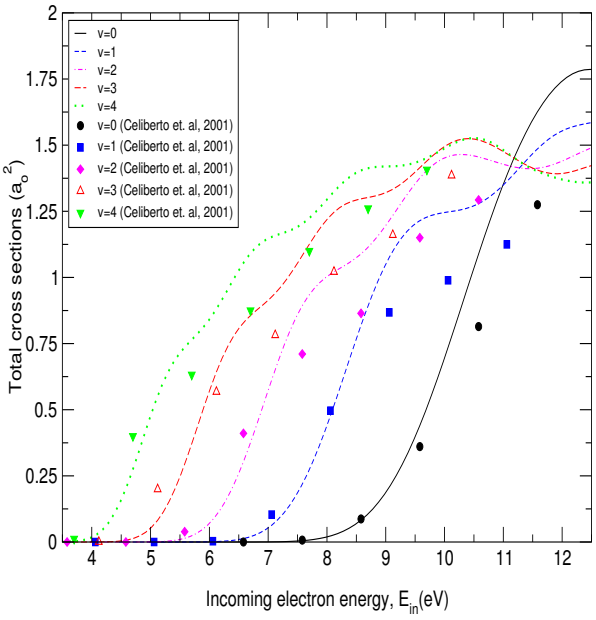

Figure 1. Electron impact dissociation cross sections for H_2 as a function of the incoming electron energy, E_{in} and initial vibrational level v obtained from our full T-matrices calculations.

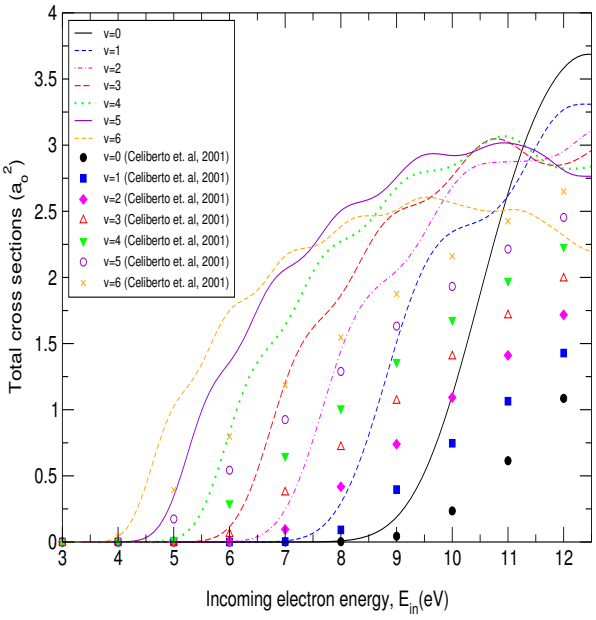

Figure 2. Electron impact dissociation cross sections for D_2 as a function of the incoming electron energy, E_{in} and initial vibrational level v obtained from our full T-matrices calculations.

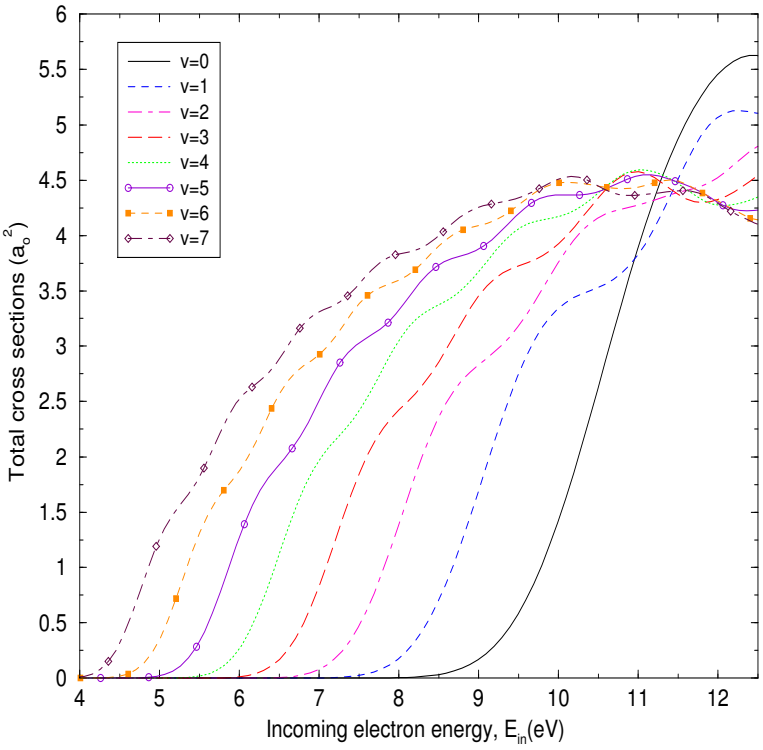

Figure 3. Electron impact dissociation cross sections for T_2 as a function of the incoming electron energy, E_{in} and initial vibrational level v obtained from our full T-matrices calculations.

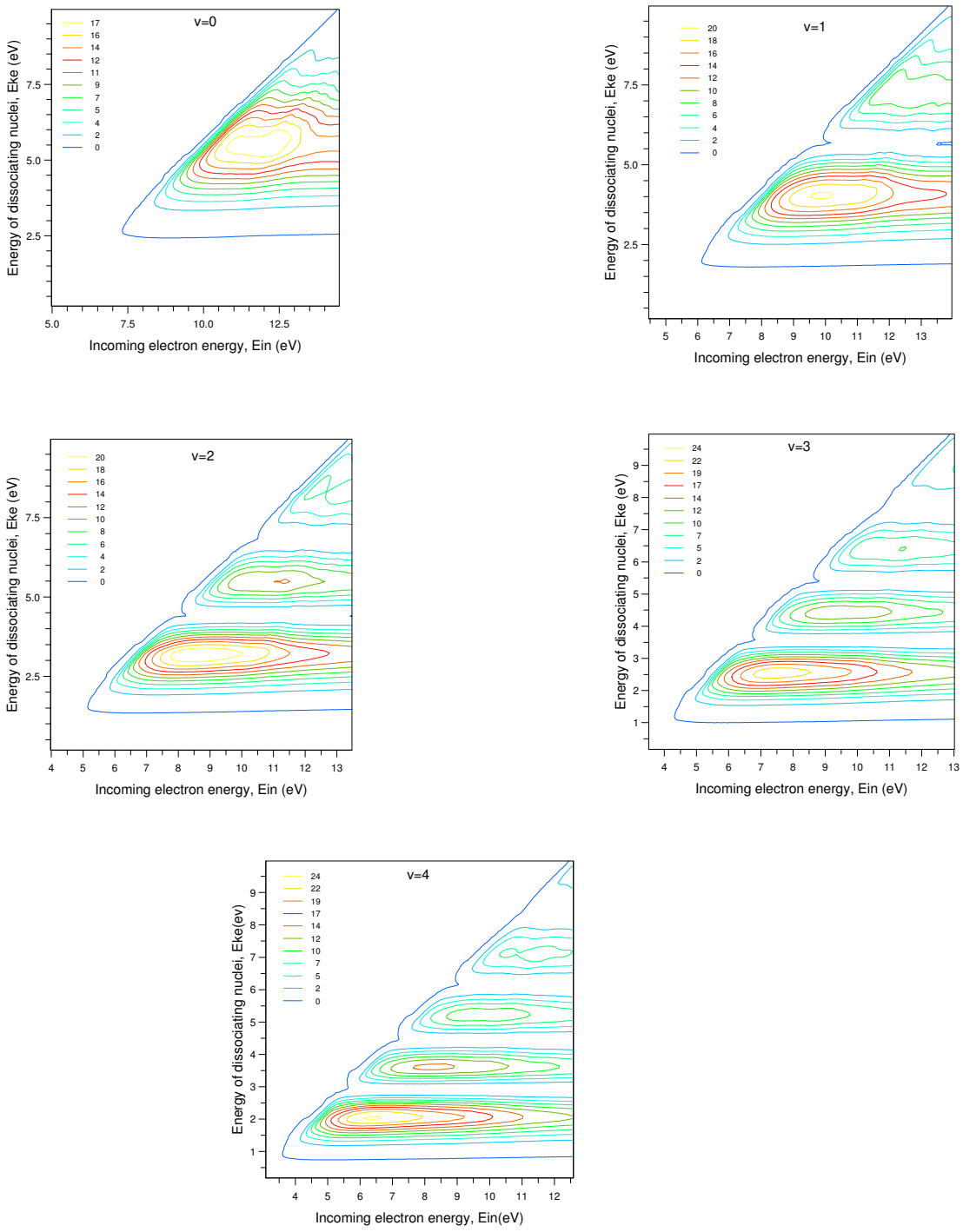

Figure 4. Energy differential cross sections electron impact dissociation of H_2 contour plot for vibrational state $v = 0 - 4$ in atomic units. The energy of the dissociating atoms, E_{ke}, is plotted against the different values of incoming electron energies, E_{in}. The structure of the bound vibrational wavefunction can be seen as v increases from $v = 0$ to $v = 4$ (left to right and top to bottom).

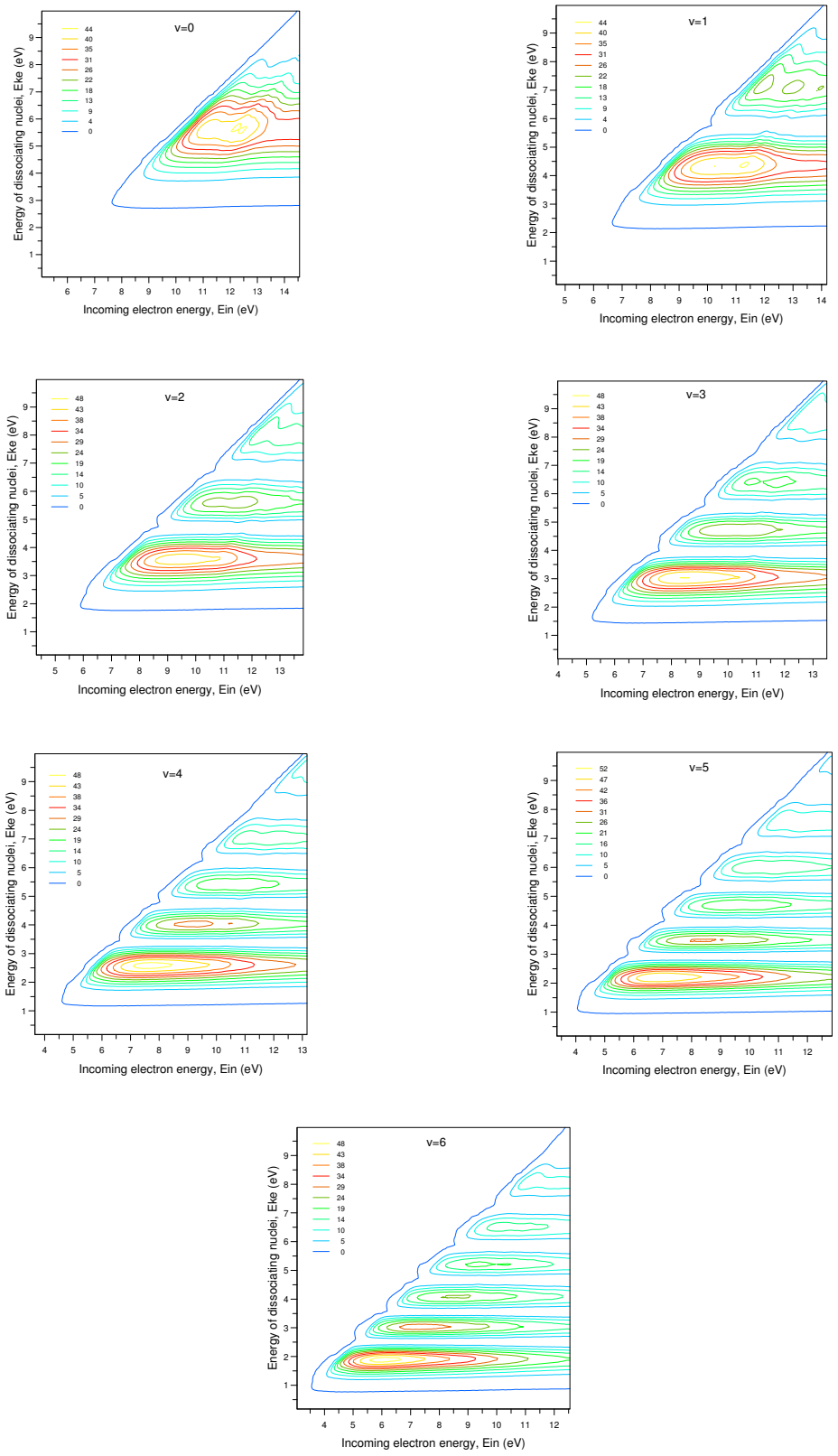

Figure 5. Energy differential cross sections electron impact dissociation of D_2 contour plot for vibrational state $v = 0 - 6$ in atomic units. The energy of the dissociating atoms, E_{ke}, is plotted against the different values of incoming electron energies, E_{in}. The structure of the bound vibrational wavefunction can be seen as v increases from $v = 0$ to $v = 6$ (left to right and top to bottom).

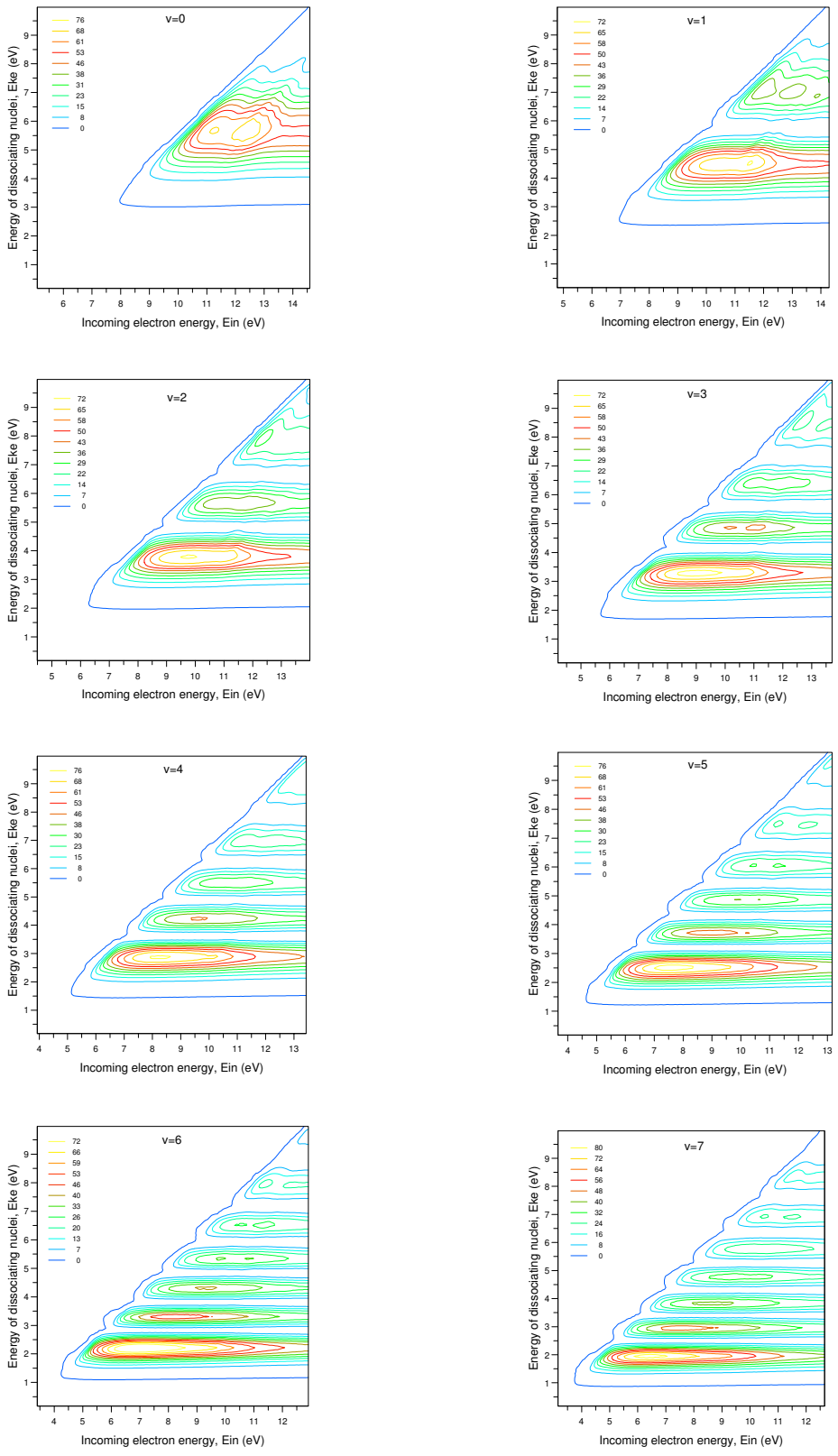

Figure 6. Energy differential cross sections electron impact dissociation of T_2 contour plot for vibrational state $v = 0 - 7$ in atomic units. The energy of the dissociating atoms, E_{ke}, is plotted against the different values of incoming electron energies, E_{in}. The structure of the bound vibrational wavefunction can be seen as v increases from $v = 0$ to $v = 7$ (left to right and top to bottom).

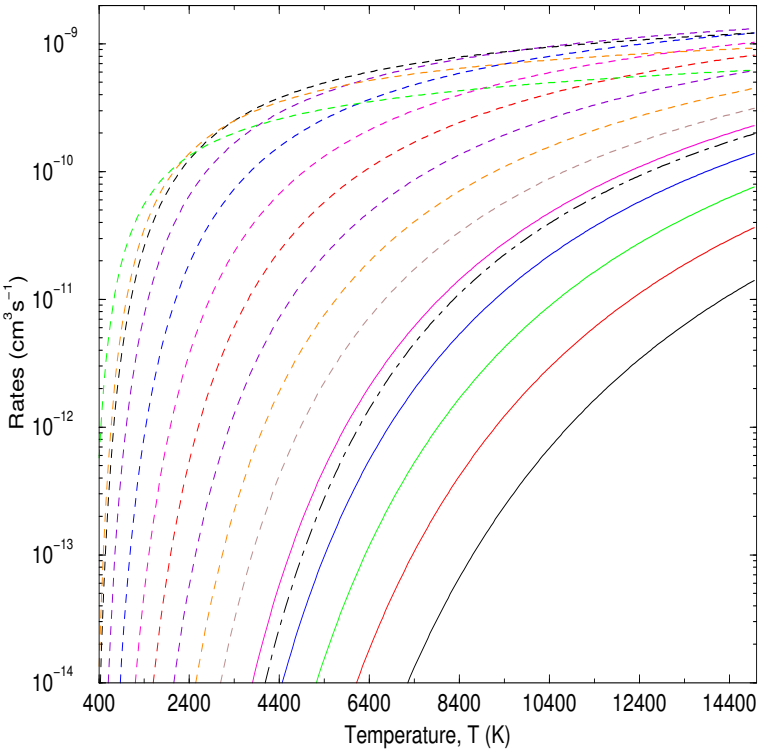

Figure 7. Electron impact dissociation rates as a function of initial H_2 vibrational state v. Full curves from the bottom are the rates for $v = 0 - 4$, obtained from our full T-matrices calculations. Broken curves from the bottom are the rates for $v = 5 - 14$. The chain curve represents the LTE rate.

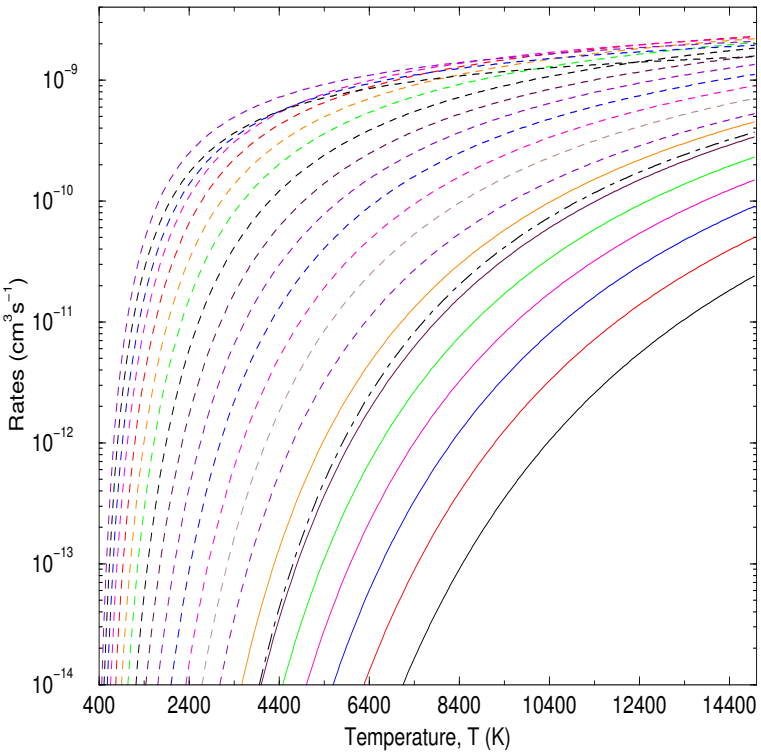

Figure 8. Electron impact dissociation rates as a function of initial D_2 vibrational state v. Full curves from the bottom are the rates for $v = 0-6$, obtained from our full T-matrices calculations. Broken curves from the bottom are the rates for $v = 7-20$. The chain curve represents the LTE rate.

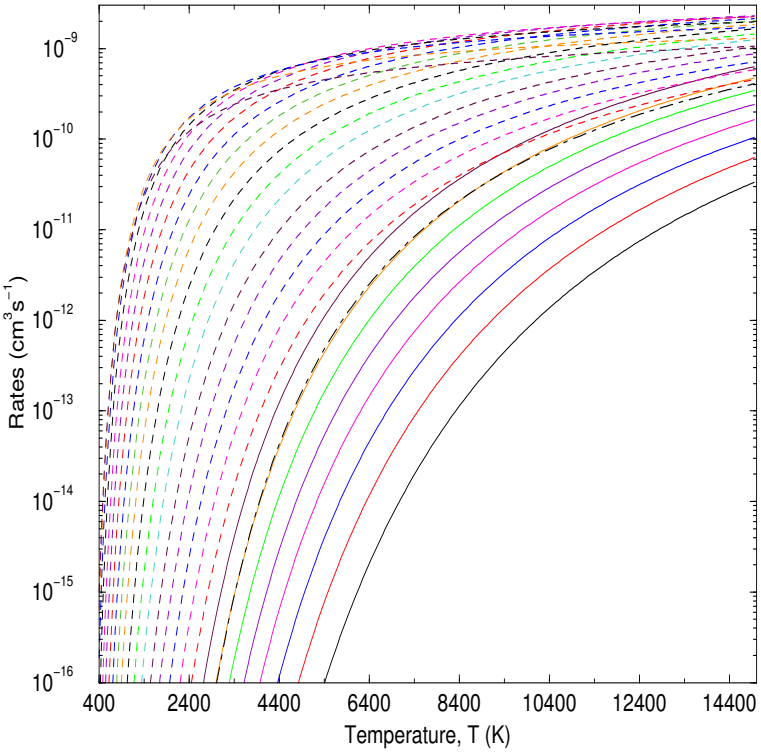

Figure 9. Electron impact dissociation rates as a function of initial T_2 vibrational state v. Full curves from the bottom are the rates for $v = 0 - 7$, obtained from our full T-matrices calculations. Broken curves from the bottom are the rates for $v = 8 - 25$. The chain curve represents the LTE rate.